Investigation of the photothermal properties of a large series of Metal-Bis(Dithiolene) complexes: Impact of the molecular structure and ranking using the photothermal index IPT

Jean-Baptiste Pluta, Nathalie Bellec, Franck Camerel

Dyes and Pigments 226 (2024) 112130

Contents lists available at ScienceDirect

Dyes and Pigments

journal homepage: www.elsevier.com/locate/dyepig

Investigation of the photothermal properties of a large series of metal-bis (dithiolene) complexes: Impact of the molecular structure and ranking using the photothermal index I_{PT}

Jean-Baptiste Pluta, Nathalie Bellec, Franck Camerel *

Institut des Sciences Chimiques de Rennes CNRS-UMR 6226, Université de Rennes, Rennes, France

ARTICLE INFO

Keywords:
Metal-bis(dithiolene)
Absorption
Photothermal index
Brilliance
Photothermal efficiency
Ranking

ABSTRACT

The photothermal properties in the NIR region of a large series of 19 metal-bis(dithiolene) complexes and of a perylene derivative have been studied in detail. Photophysical and thermal measurements were repeated several times to obtain good uncertainties on molar extinction coefficients, temperature increases and photothermal efficiencies. This large series of metal-bis(dithiolene) complexes enabled us to assess the impact of the nature of the metal center, the nature of the ligand and the number and length of the carbon chains on absorption properties and photothermal efficiencies. Thanks to these reliable data, the recently introduced photothermal index I_{PT}, which combines molar absorptivity ε and photothermal efficiency η, has also been effectively used to rank all these molecular photothermal agents according to their photothermal activity. This work confirms that the photothermal index I_{PT} can be used effectively to rank photothermal agents according to their ability to convert light into heat.

1. Introduction

Photothermal therapy (PTT), a cutting-edge approach in medical treatment, harnesses the power of light to target and destroy diseased cells [1,2]. By utilizing materials that efficiently absorb near-infrared (NIR) light, this therapy selectively heats targeted tissues, leading to their eradication while sparing healthy surrounding cells. The near-infrared region, with wavelengths ranging from 700 to 1700 nm, is particularly advantageous for photothermal therapy due to its ability to penetrate deeper into biological tissues with minimal absorption and scattering [3–5]. The NIR window can be divided into two wavelength regions: NIR-I (700–950 nm) and NIR-II (1000–1700 nm) [6]. Photothermal agents (PTAs) absorbing in the NIR-II region allow for deeper penetration length and higher contrast in living tissues. This characteristic enables precise targeting of tumors and other pathological sites located deep within the body. Moreover, the non-invasive nature of NIR light allows for precise control and monitoring during treatment, minimizing damage to adjacent healthy tissues. As research in this field advances, photothermal therapy holds promise for revolutionizing cancer treatment and combating various diseases with unparalleled precision and efficacy. However, normal or malignant tissues lack of efficient photothermal activity and exogenous NIR absorbents are often used for facilitating efficient heat production. Several exogenous agents have been explored for their photothermal activity in the NIR region. These agents can vary from gold nanoparticles [7], carbon nanotubes [8], graphene oxide [9], Prussian blue nanocubes [10], hybrid nanosystems [11], conjugated polymers [12] transition metal dichalcogenides (TMDs) [13], upconversion nanoparticles … [14] However, considering the translation of NIR PTAs into clinical applications, small molecules remain the most desirable and optimal candidates because of their high biocompatibility, fast excretion, quality control under the current Good Manufacturing Practice (cGMP) conditions, and easy and robust preparation. Molecular cyanine dyes are popular small molecule NIR-II photothermal agents. However, their isolation requires an intensive synthetic work and their absorption maxima hardly exceed 1100 nm [15–17]. Therefore, developing small molecule based NIR PTAs with desirable chemical and physical properties, favourable excretion pharmacokinetics, minimal cellular toxicity and clinical translation ability is crucial and highly demanded.

However, another important factor to consider is the PTA's ability to efficiently convert light into heat. Indeed, the more effective the molecular PTA, the less product needs to be introduced into the human body to reach the desired hyperthermia temperature, thus limiting undesirable side effects during treatment. It is therefore important to be

* Corresponding author.
E-mail address: franck.camerel@univ-rennes.fr (F. Camerel).

https://doi.org/10.1016/j.dyepig.2024.112130
Received 6 March 2024; Received in revised form 28 March 2024; Accepted 29 March 2024
Available online 30 March 2024

able to select the most effective photothermal agents from an arsenal of potentially useable compounds in order to limit the doses to be injected and the undesirable side effects. By prioritizing agents with higher conversion efficiencies, treatment outcomes can be optimized, ensuring maximal destruction of diseased tissues while minimizing damage to healthy cells. This means that in addition to assessing their toxicity, we need to be able to correctly rank agents according to their photothermal activity. This ranking process will facilitate the development of more precise and efficient treatment protocols, enhancing therapeutic efficacy and patient outcomes. Additionally, ranking agents based on photothermal efficiency fosters innovation and encourages the design of novel materials with enhanced photothermal properties, driving progress in medical science and technology.

Recently, we have defined a new physical parameter, the photothermal index I_{PT}, comparable to the brilliance in luminescence, which allow to properly rank molecular photothermal agents as a function of their ability to convert light into heat, with minimal experimental constraints [18]. It has been shown that the photothermal efficiency (or the photothermal yield) η or the molar extinction coefficient ε alone cannot account for the temperature increase that can be generated for a given laser power. However, it has been shown that the temperature increase is directly proportional to the product of the photothermal efficiency η and the molar extinction coefficient ε, which defines the photothermal index (photothermal brilliance). Knowing the photothermal index of a compound, it's thus easy to determine whether it will produce more or less heat than another compound at the same molar concentration, by comparing their respective indices. However, the demonstration that the temperature increase under laser irradiation is linearly proportional to this photothermal index was only performed on a limited number of photothermal agents.

Metal-bis(dithiolene) are stable and effective photothermal agents under NIR laser irradiation, and their photothermal properties have been exploited in a variety of technological applications ranging from photothermal therapy and photocontrolled drug delivery to optical data storage and soft robotics [19]. Recently, neutral d^8 metal-bis(dithiolene) complexes have also been used for solar-stream generation [20].

To further improve the photothermal index, we have conducted a new study on a larger series of metal-bis(dithiolene) complexes (Scheme 1). In the present work, we have investigated the photothermal properties of nineteen metal-bis(dithiolene) complexes (**M(dt$_2$)**) with different metal centers and different ethene-1,2-bis(thiolate) or 1,2-diphenylethene-1,2-bis(thiolate) ligands carrying alkoxy chains in various positions, in order to evaluate the impact of the molecular structure on their ability to convert light into heat. Photophysical and photothermal measurements were repeated several times to obtain good uncertainties on molar extinction coefficients, temperature increases and photothermal efficiencies, to determine the photothermal index of each complex with good confidence. For comparison with other molecular systems, these measurements were also carried out on a perylene derivative (**PerDIS**), recently studied for its photothermal properties in the NIR region [18].

2. Results and discussions

The nineteen metal-bis(dithiolene) complexes selected for this study are presented in Scheme 1. Four dithiolene complexes were formed by complexation of two diphenylethylenedithiolate ligands bearing four C4 carbon chains with nickel, platinum, palladium and gold as metal center (**M4(OC4)**). Four dithiolene complexes were formed by complexation of two diphenylethylenedithiolate ligands bearing four C12 carbon chains (**M4(OC12)**) with M = Ni, Pd, Pt and Au. Four dithiolene complexes were obtained by complexation of two diphenylethylenedithiolate ligands bearing eight C12 carbon chains in 3,4 positions (**M8(OC12)**) with M = Ni, Pd, Pt and Au. Two parent nickel complexes with a methoxy substitution in the *para* position **Ni4(OMe)** and without any substituent **Ni4Ph** on diphenylethylenedithiolate ligands were also added. These series will enable us to study the impact of the metal center and alkoxy substitution on diphenylethylenedithiolate ligands on absorption and photothermal properties. Three nickel complexes with *n*-alkylthio-substituted ethylene-1,2dithiolate ligand **M(dmitCn) n = 4, 8, 12** were also added to these series to study the impact of the nature of the ligand and of the carbon chain length on the photothermal efficiency. Two gold complexes, **Au(D-bordt)** and **Au(DL-bordt)**, described in the literature, were also added to further study the impact of the nature of the dithiolene ligand on photothermal properties [21]. This large series of **M(dt$_2$)** complexes, which are now well-known and highly stable PTAs, will thus enable us to study the role of the dithiolene ligand, the metal center and the carbon chains on the photophysical and photothermal properties. For comparison, one PTA of completely different structure was also finally studied. A sulfurated perylene derivative (**PerDIS**) absorbing in the NIR region have been integrated into this study [22]. Several equimolar solutions of each compound (10^{-5} mol L^{-1}) have been prepared in toluene. Toluene was chosen as the solvent because it combines the advantages of being hydrophobic (making it a good solvent for our complexes) and having a high boiling temperature (110 °C at atmospheric pressure), which will be of interest for photothermal studies.

The absorption spectrum of each solution was recorded between 320 and 1650 nm on a Shimadzu UV-3600 Plus spectrophotometer at a concentration of 10^{-5} mol L^{-1} (Detection limit = 1650 nm in toluene with a quartz cuvette). All measurements were carried out under equimolar conditions to facilitate comparison of the complexes. Several solutions of each complex were prepared to obtain good uncertainties on the molar extinction coefficients. λ_{max} at the absorption maximum and associated molar absorption coefficients ε_{max} are gathered in Table 1.

The spectra of **M4(OC12)** compounds with M = Ni, Pd, Pt and Au are shown in Fig. 1. It can be seen that for identical ligands, the metal center has a strong influence on the absorption maximum wavelength λ_{max} of the complex and on the shape of the absorption band. The **Ni4(OC12)** and **Pd4(OC12)** complexes have close absorption maxima at 929 and 950 nm, respectively. The absorption maximum for **Pt4(OC12)** is located at a slightly lower wavelength (866 nm), while **Au4(OC12)** has an absorption maximum located well within the NIR-II region at 1568 nm. For M = Ni/Pd/Pt, λ_{max} remains confined to a fairly narrow wavelength range in the NIR-I region, while the absorption maximum is well within the NIR-II region for M = Au. The significant bathochromic shift observed in the case of the gold complex is due to its radical nature, which strongly reduces the electronic gap between the B_{1u} and B_{2g} frontier orbitals [21]. The second consequence of the change of metal concerns the intensity of absorption, quantified by the molar absorptivity. The molar absorptivity at absorption maximum (ε_{max}) of the palladium and platinum complexes is fairly close, at 55070 and 59180 L mol^{-1} cm^{-1}, respectively. For the nickel complex, a slight hypochromic effect is observed and the molar absorptivity decreases to 40455 L mol^{-1} cm^{-1}. However, for the gold complex, this hypochromic effect is much more pronounced and the molar absorptivity is almost half that of the platinum complex (ε_{max} = 27395 L mol^{-1} cm^{-1}). The same observations can be done for the **M4(OC4)** and **M8(OC12)** series, whose spectra can be found in supporting information (Figs. S1 and S2).

The absorption spectra of nickel complexes with the various 1,2-diphenylethene-1,2-bis(thiolate) ligands are shown in Fig. 2, enabling us to study the impact of alkoxy substitution on absorption properties. The **Ni4Ph** complex, devoid of any alkoxy substitution, absorbs at 858 nm. The introduction of an alkoxy chain in the *para* position, including methoxy substitution, induces a ~70 nm batochromic shift in the absorption band. This shift is attributed to the donor effect imported by the alkoxy group. Increasing chain length from C1 to C12 does not affect peak position, but a clear hyperchromic effect is observed from C1 to C4. Above C4, chain length does not affect the molar absorptivity of the complex. The introduction of an additional alkoxy chain in position 3 further shifts the absorption band from ~32 nm to higher wavelengths.

The absorption properties of the three **Ni(dmitCn)** complexes are remarkably similar (Table 1 and Fig. 3). They have the same absorption

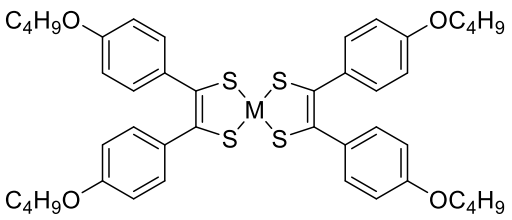

M4(OC4)
M= Ni, Pt, Pd, Au

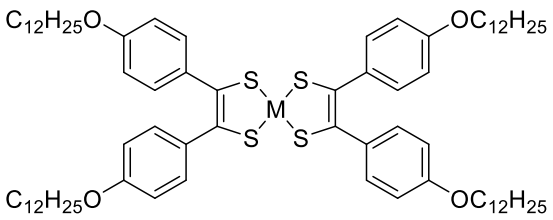

M4(OC12)
M= Ni, Pt, Pd, Au

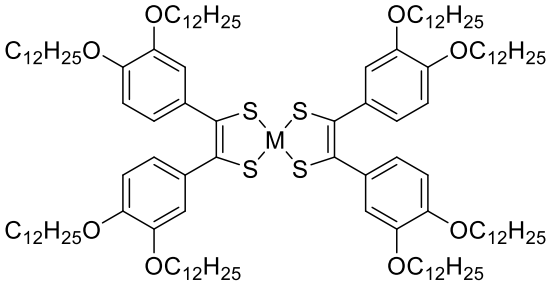

M8(OC12)
M= Ni, Pt, Pd, Au

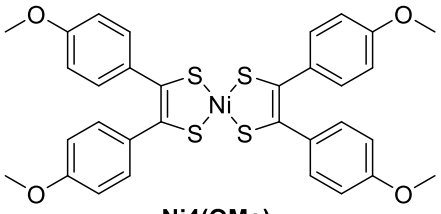

Ni4(OMe)

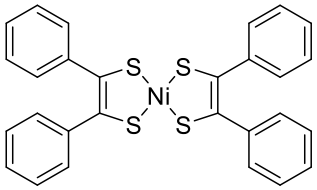

Ni4Ph

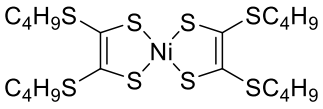

Ni(dmitC4)

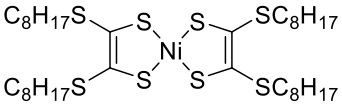

Ni(dmitC8)

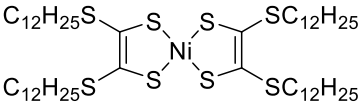

Ni(dmitC12)

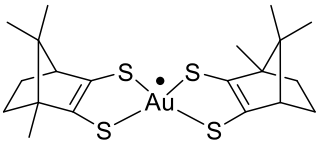

Au(D-bordt)

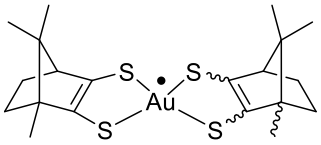

Au(DL-bordt)

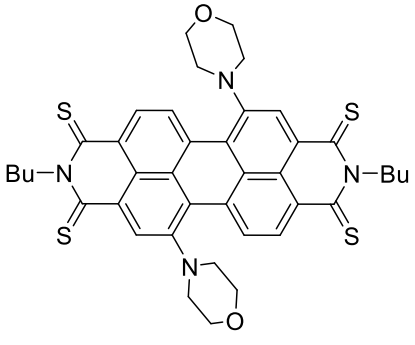

PerDIS

Scheme 1. List of the photothermal agents investigated in this study.

Table 1
Values of λ_{max} and ε_{max} with its Student interval in toluene for each complex (C = 10^{-5} mol L^{-1}, N is the number of measurements performed).

Complex	λ_{max} (nm)	ε_{max} (L.mol^{-1}.cm^{-1})	N
Ni4(OC4)	929	39505 ± 270	3
Ni4(OC12)	929	40455 ± 310	6
Ni8(OC12)	961	38770 ± 785	6
Pd4(OC4)	950	46200 ± 1740	3
Pd4(OC12)	950	55070 ± 480	6
Pd8(OC12)	983	41800 ± 405	3
Pt4(OC4)	866	52340 ± 810	6
Pt4(OC12)	866	59180 ± 660	6
Pt8(OC12)	897	52580 ± 130	6
Au4(OC4)	1568	25535 ± 690	6
Au4(OC12)	1568	27395 ± 130	6
Au8(OC12)	1614	17440 ± 450	6
Au(D-bordt)	1500	17190 ± 370	6
Au(DL-bordt)	1500	17590 ± 90	6
Ni4(OMe)	924	30720 ± 1825	3
Ni4Ph	858	31100 ± 280	2
Ni(dmitC4)	1010	36430 ± 320	3
Ni(dmitC8)	1010	38640 ± 270	6
Ni(dmitC12)	1010	38970 ± 550	6
PerDIS	852	22470 ± 650	3

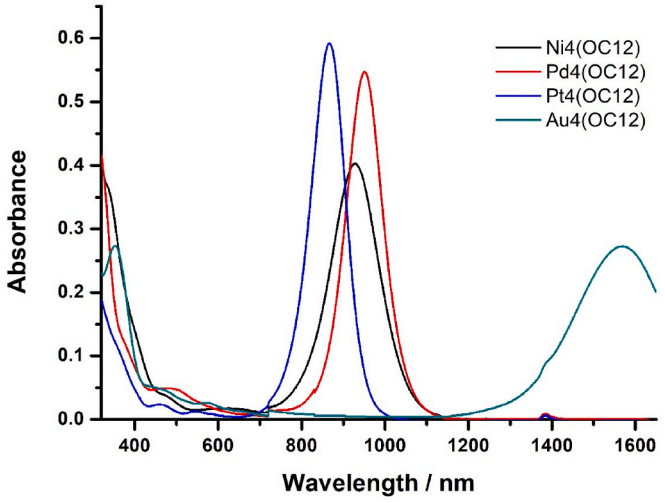

Fig. 1. Absorption spectra of **M4(OC12)** complexes at 10^{-5} mol L^{-1} in toluene, 320–1650 nm. The small peak observed around 1400 nm is an artefact due to the change of lamps. Detection limit = 1650 nm in toluene with a quartz cuvette (The artefact observed at 720 nm is due to the lamp change).

maximum at λ_{max} = 1010 nm which is not affected by the chain length. Compared to the **Nix(OCn)** complexes, only a slight hyperchromic effect of ~2000 L mol^{-1} cm^{-1} is observed going from C4 to C8 and the molar absorptivities of **Ni(dmitC8)** and **Ni(dmitC12)** are very close around 38800 L mol^{-1} cm^{-1}. This shows that for this ligand structure, absorption properties are weakly affected by the length of the thioalkyl chain (at least in the case of nickel). Compared with **Nix(OCn)** complexes, **Ni(dmitCn)** shows a higher λ_{max}, for a similar ε_{max}. It would have been

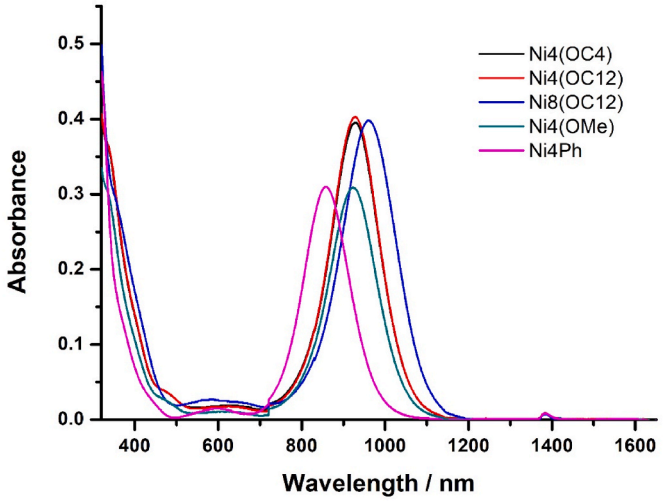

Fig. 2. Absorption spectra of the three **Nix(OCn)** complexes versus **Ni4(OMe)** and **Ni4Ph**, at 10^{-5} mol L^{-1} in toluene, 320–1650 nm (The artefact observed at 720 nm is due to the lamp change).

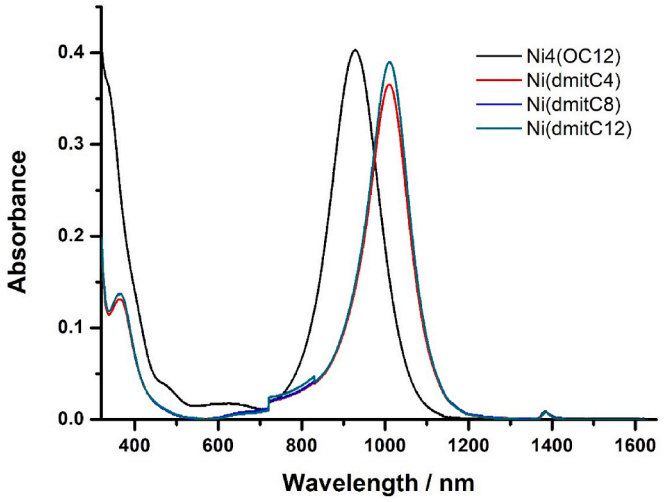

Fig. 3. Absorption spectra of the three **Ni(dmitCn)** compared with **Ni4(OC12)**, at 10^{-5} mol L^{-1} in toluene, 320–1650 nm (spectra of **Ni(dmitC8)** and **Ni(dmitC12)** are superimposed) (The artefact observed at 720 nm is due to the lamp change).

interesting to diversify the metal centers of these complexes to see if our observations in the case of nickel remain valid for other metals (as the **Mx(OCn)** with Pd, Pt and Au show more variability between them at identical ligands). Unfortunately, obtaining these dmit complexes with other metal centers proved to be particularly capricious and laborious.

Finally, the absorption spectra of gold complexes are shown in Fig. 4. As already mentioned, due to their radical character, these complexes absorb far into the NIR-II region [23]. The absorption spectra of **Aux(OCn)** complexes show a strong absorption band centered at 1600 nm and at 1500 nm for **Au(bordt)** complexes, showing that the position of the absorption band is strongly influenced by the nature of the dithiolene ligand. Conclusions concerning the variation of λ_{max} as a function of the number and length of alkyl chains are the same for **Aux(OCn)** as for the **Nix(OCn)** series. The change from one chain in *para* position to two chains in positions 3 and 4 increases λ_{max} ($\Delta\lambda$ = +46 nm, slightly more than the additional 30 nm for M = Ni/Pd/Pt). In contrast to **Nix(OCn)**, there are disparities on ε_{max} (also observed on palladium). In the case of chiral complexes, there is no difference in absorption properties

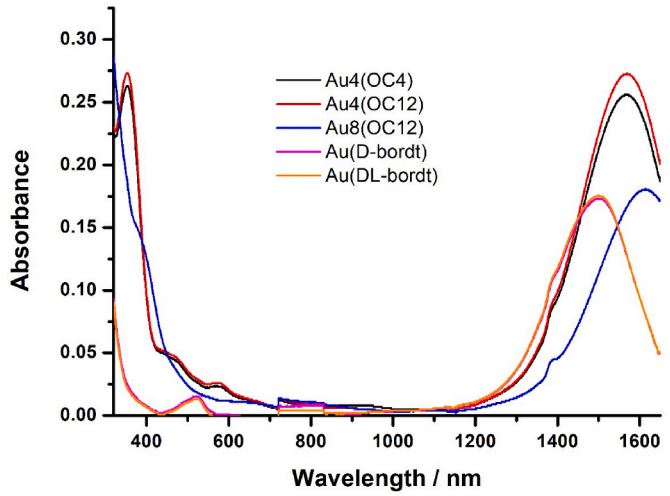

Fig. 4. Absorption spectra of the five **Au(dt)$_2$**, at 10^{-5} mol L^{-1} in toluene, 320–1650 nm. Detection limit = 1650 nm in toluene with a quartz cuvette (The artefact observed at 720 nm is due to the lamp change).

depending on whether the complex is optically pure or racemic (λ_{max} of 1500 nm and ε_{max} of ~17400 L mol^{-1} cm^{-1}). Comparing all our **Au(dt)$_2$**, we observe that the sum of their absorption domains covers the second half of the NIR-II region. However, their absorption intensity remains lower than that of all other Ni/Pd/Pt complexes in the NIR-I region.

All nineteen dithiolene complexes in this chemical library have intense absorption in the NIR. **M(dt)$_2$** with M = Ni/Pd/Pt have their absorption maxima in the NIR-I whereas the **Au(dt)$_2$** absorb in the NIR-II region. However, the gold complexes have a less intense absorption. Modifying the electron-donating effect on the ligands by means of substituents (in this case alkoxy chains) enables absorption properties to be modified quite finely (on λ_{max} and ε). In this way, the absorption maximum can be finely tuned by correctly selecting the metal center, the dithiolene ligand and its substitution pattern from 800 nm up to 1650 nm.

The photothermal properties of the dithiolene complexes were investigated on equimolar solutions in toluene by monitoring the temperature profile during 18 min under continuous laser irradiation at 880, 940 or 1600 nm at 3 W cm^{-2}, depending on absorption maximum of the dithiolene complexes, and for 18 min after turning off the laser. At a concentration as low as 10^{-5} mol L^{-1}, 3 W cm^{-2} was found to be a good compromise for measuring a significant temperature rise without reaching the solvent boiling point. From now on, the sequence of a heating phase immediately followed by a cooling phase (or laser on and laser off respectively) will be called the ON-OFF cycle. Representative temperature profiles are presented in Fig. 5 and in supporting information (Figs. S3–S21 left). It was found that it was necessary to irradiate for 18 min in order to properly reach the steady-state regime. Table 2 below shows the absorption maximum wavelength λ_{max}, the irradiation wavelength λ_{laser}, the maximum temperature T_{max} and the calculated photothermal yield η for all the complexes. All these measurements were performed on 10^{-5} mol L^{-1} complex solutions in toluene, irradiated at 3 W cm^{-2}. The photothermal conversions efficiencies (η) were extracted from the recorded temperature profiles. The η values were calculated as described earlier, according to the equation reported by Roper et al. [24]. Full details are given in SI and the η values are gathered in Table 2.

Within the **Mx(OCn)** series, **M8(OC12)** complexes have the highest efficiency η, indicating that the increase of the number of the carbon chains increase the photothermal conversion efficiency. Regarding the temperature increase, the platinum and the palladium complexes appears to be more efficient PTAs than the nickel complexes. The gold complexes, despite absorbing the NIR-II region are less efficient PTAs. Interestingly, it can be observed that the complexes displaying the highest photothermal efficiencies do not necessary lead to the highest temperature increases. As an example, **Pd4(OC12)** complex with a photothermal efficiency of 43.3 % show a higher temperature increase (T_{max} = 100.6 °C) than **Pd8(OC12)** with a photothermal efficiency of 56.4 % which only reaches a T_{max} of 89.2 °C. Two complexes can have very similar T_{max} and η values (**Ni4(OC4)** and **Ni4(OC12)**), have the same T_{max} and different η values (**Pt4(OC12)** and **Pt8(OC12)**), or have different T_{max} values for the same η value (**Au4(OC12)** and **Au8(OC12)**). This is even true by comparing with the **Ni(dmitCn)** and the **Aubordt** series. These complexes display the highest photothermal efficiencies but the maximum temperature only reaches ~70 °C.

The impact of alkyl chain length on photothermal efficiency is unclear. If we look at the **M4(OCn)** series, we find that C4 chains can lead to higher efficiencies than C12 chains, and vice versa. The same applies to the **Ni(dmitCn)** series, where C8 chains give higher photothermal efficiencies than C4 or C12 chains. The only certainty is that C4 and C12 chains are in both cases better than a methyl group alone.

Focusing on nickel as the metal center, a certain homogeneity of the values of T_{max} and η for **Nix(OCn)** can be observed (~89 °C and ~46 %). This homogeneity is found for **Ni(dmitCn)** but only on T_{max} (~70.2 °C). The η values are significantly more dispersed for **Ni(dmitCn)** complexes (from 56.5 to 64.2 %). This greater variability may be due to the

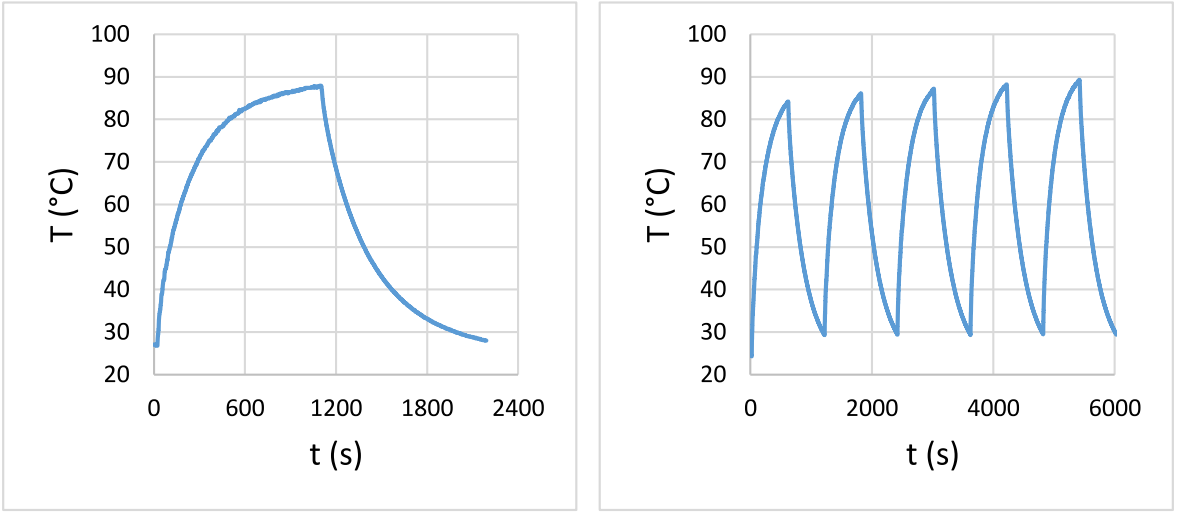

Fig. 5. Photothermal measurements for **Ni4(OC4)** at 940 nm. ON-OFF cycle at 3 W cm^{-2}, t_{ON} = 18 min (left) and thermal stability at 5 W cm^{-2} (right).

Table 2
Quantitative photothermal values for all the complexes dissolved at 10^{-5} mol L^{-1} in toluene. Irradiation at 3 W cm^{-2}. N is the number of measurements performed. (*The uncertainty is not indicated because the dispersion is too large).

Complex	λ_{max} (nm)	λ_{laser} (nm)	T_{max} (°C)	η (%)	N	$I_{PT\lambda laser}$
Ni4(OC4)	929	940	88.1 ± 0.8	45.5 ± 1.3	3	17.5 ± 0.5
Ni4(OC12)	929	940	87.8 ± 1.0	45.0 ± 1.0	6	17.8 ± 0.4
Ni8(OC12)	961	940	91.1 ± 1.0	48.0 ± 1.9	3	17.6 ± 0.8
Pd4(OC4)	950	940	94.6 ± 0.7	44.4 ± 2.1	3	19.9 ± 1.2
Pd4(OC12)	950	940	100.6 ± 0.5	43.3 ± 1.1	6	23.1 ± 0.6
Pd8(OC12)	983	940	89.2 ± 4.3	56.4 ± 4.7	3	15.9 ± 1.4
Pt4(OC4)	866	880	93.9 ± 1.7	32.3 ± 1.3	6	15.9 ± 0.7
Pt4(OC12)	866	880	100.8 ± 0.8	35.9 ± 1.0	6	20.0 ± 0.6
Pt8(OC12)	897	880	102.6 ± 0.7	39.3 ± 1.4	6	19.4 ± 0.7
Ni(dmitC4)	1010	940	69.3 ± 1.0	56.5 ± 3.5	3	9.5 ± 0.6
Ni(dmitC8)	1010	940	71.4 ± 1.2	64.2 ± 3.7	3	11.2 ± 0.7
Ni (dmitC12)	1010	940	70.1 ± 0.9	57.3 ± 9.6	3	10.1 ± 1.7
Ni4(OMe)	924	940	75.2*	39.5*	2	11.5 ± 0.1
Ni4Ph	858	880	67.0 ± 0.7	30.6 ± 3.2	3	8.7 ± 0.9
Au4(OC4)	1568	1600	79.8 ± 3.1	39.4 ± 3.9	6	9.6 ± 1.0
Au4(OC12)	1568	1600	82.4 ± 3.5	40.3 ± 3.8	6	10.5 ± 1.0
Au8(OC12)	1614	1600	69.8 ± 3.2	41.1 ± 4.1	6	7.1 ± 0.7
Au(D-bordt)	1500	1600	67.5 ± 0.9	66.4 ± 1.2	6	6.1 ± 0.2
Au(DL-bordt)	1500	1600	67.6 ± 0.4	63.5 ± 2.0	6	6.0 ± 0.2
PerDIS	852	808	59.5 ± 0.9	36.0 ± 1.4	3	8.1 ± 0.55
PerDIS	852	880	57.1 ± 1.55	24.1 ± 1.3	3	5.4 ± 0.4

different structure of the ligands, or to the fact that **Ni(dmitCn)** are irradiated farther from their λ_{max}, 70 nm compared to 20 nm or less for **Nix(OCn)**. **Ni4(OMe)** appears to be the less efficient photothermal agent of the **Nix(OCn) series**. Finally, **Ni4Ph** is the worst performing nickel complex with an average yield η of "only" 30.6 %. Among diphenylethylenedithiolate ligands, the strategy to adopt to maximize T_{max} and η is thus to substitute each aromatic ring with as many alkoxy chains as possible, themselves the longest possible. Indeed, by adding more and more longer carbon chains, the sequence **Ni4Ph → Ni4(OMe) → Ni4(OC4) → Ni4(OC12) → Ni8(OC12)** for increasing values of T_{max} and η is obtained.

Focusing now on the gold complexes, **Au8(OC12)** shows a photothermal yield similar to **Au4(OC4)** and **Au4(OC12)**, although having a lower equilibrium temperature of about 10 °C. The two bordt ligand complexes show a maximum temperature similar to **Au8(OC12)** and the highest photothermal efficiencies in the **Au(dt)$_2$** series (64 % *vs.* 40 %). We can assume that the T_{max} would be higher if we had a laser more suitable for irradiation. Indeed, the 1600 nm laser is located close to the λ_{max} of **Aux(OCn)** (1568 and 1614 nm, i.e. 32 and 14 nm from the λ_{laser}), but the difference with the λ_{max} of **Au(D/DL-bordt)** is 100 nm which is much more important (we are almost half-way the absorption maximum). As for the absorption properties, it is observed that the chirality of the ligands has no influence on the photothermal properties.

All the dithiolene complexes were found to be highly photothermally stable. No fatigue was observed after several heating and cooling cycles even under 5 W cm^{-2} power laser irradiation (Fig. 5, S3-S20 right).

As demonstrated, the photothermal agent with the highest photothermal efficiency do not necessary lead to the highest temperature increases, meaning that the molecules displaying the highest conversion efficiencies are not necessary the best PTA, i.e. the PTA producing the most heat under laser irradiation. The temperature increase depends on the photothermal conversion efficiency of the compound but also on its molar extinction coefficient at the irradiation wavelength. The temperature increase with a compound that strongly absorbs the laser and has a good photothermal efficiency will be much higher than that with a compound that has a low absorption and a low ability to convert light into heat. Thus, to be considered as a good photothermal agent, the compound should strongly absorb at the irradiation wavelength and should also display a high photothermal conversion efficiency. As a consequence, the photothermal efficiencies are not sufficient to rank the PTAs between them. For these reasons, in order to better rank the molecular PTAs, the new photothermal index (I_{PT}) strongly resembling the brilliance in fluorescence, which accounts for both the absorption coefficient and the photothermal yield, has been recently introduced [18].

The I_{PT} is defined as follows:

$$I_{PT\lambda} = \varepsilon_\lambda \text{ x } \eta \text{ x } 10^{-5} \qquad \text{(Equation 1)}$$

where ε_λ is the molar absorptivity at the irradiation wavelength λ (ε_λ in $L.mol^{-1}.cm^{-1}$ and η in %). $I_{PT\lambda}$ was multiplied by a factor 10^{-5} to obtain more convenient values.

It has been demonstrated on a limited number of molecules that the increase in temperature is linearly proportional to the I_{PT}: $\Delta T_{max} = f(I_{PT})$ [18].

With a larger library of molecules at our disposal, this prompted us to further test this IPT index as an effective tool for classifying photothermal agents.

Firstly, the T_{max} of all nickel complexes was plotted against their respective I_{PT} values (Fig. 6). As can be seen, the values are perfectly distributed along a straight line. In the present study, T_{max} was used instead of ΔT_{max} as a much better linear correlation was obtained and T_{max} proved to have very low or no sensitivity to starting temperature. As expected, the molecule with the highest I_{PT} produced more heat. In the nickel complex series, the most effective photothermal agents are complexes with diphenylethylenedithiolate ligands bearing long carbon chains **Ni4(OC4)**, **Ni4(OC12)** and **Ni8(OC12)**. The worst photothermal agent is the **Ni4Ph** complex with no substituent. The **Ni4(OMe)** complex lies in between, as do the **Ni(dmitCn)** complexes for which photothermal activity increases linearly with chain length. It's also worth noting that the **Ni4Ph** complex, despite being the only one irradiated at 880 nm (compared with 940 nm for all other nickel complexes), fits very well into the line.

For the gold complexes, the values are also well distributed along a straight line (Fig. 7). **Au(D-bordt)** and **Au(DL-bordt)** have a lower photothermal activity than complexes with diphenylethylenedithiolate ligands. **Au4(OC12)** is the complex with the highest photothermal conversion activity at 1600 nm following by **Au4(OC4)** and **Au8(OC12)**.

For a better overview, all complexes have been plotted on the same Fig. 8 (Fig. S22 is given with deviations in SI). Perylene derivative values have also been added (representative temperature profile presented in

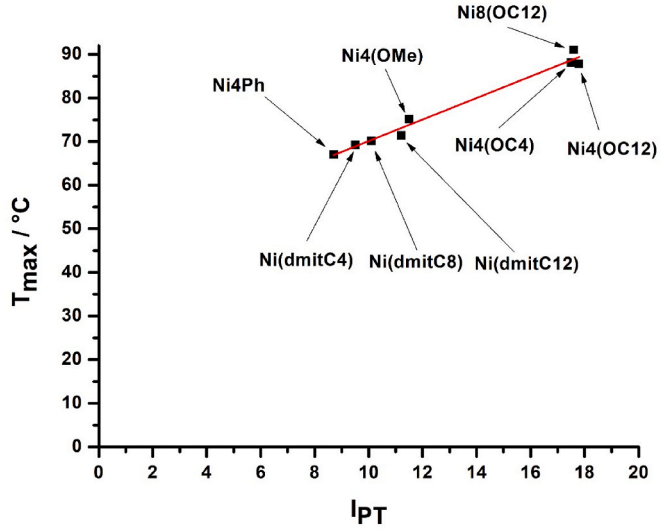

Fig. 6. Maximum temperature reached under laser irradiation as a function of I_{PT} for the nickel complexes (correlation coefficient of the linear regression R^2 = 0.9782).

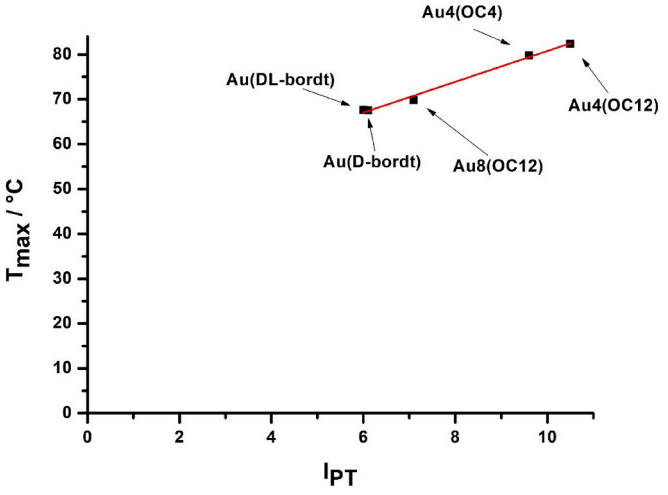

Fig. 7. Maximum temperature reached under laser irradiation as a function of I_{PT} for the gold complexes (correlation coefficient of the linear regression R^2 = 0.99).

Fig. S23). As can be seen, all values are distributed along a straight line and confirm the correlation between I_{PT} and the maximum temperature T_{max} reached under irradiation. Palladium and platinum complexes are clearly the best PTA. Depending on the nature of the ligand and their functionalization, nickel complexes are much more dispersed along the line. Nickel complexes with diphenylethylenedithiolate ligands bearing long carbon chains have a photothermal activity comparable to palladium and platinum complexes ones. The other nickel complexes have lower photothermal activity. Gold complexes are less effective photothermal agents, but it should be emphasized that they are the only photothermally active metal complexes to absorb so far in the NIR-II region. It is also clear that all dithiolene complexes are better photothermal agents than the perylene derivative. The linear correlation seems better when considering a single metal center.

3. Conclusion

In the present work, a chemical library of nineteen metal-bis (dithiolene) complexes has been characterized in order to understand

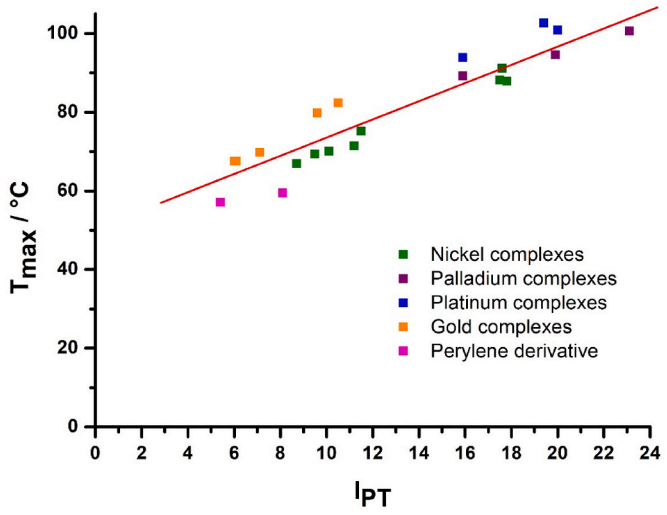

Fig. 8. Maximum temperature reached under laser irradiation as a function of I_{PT} for all the complexes (correlation coefficient of the linear regression R = 0.8724).

their photophysical and photothermal properties, which are essential in the context of PTT. All the nickel, palladium and platinum **M(dt)$_2$** complexes absorb in the NIR-I region (650–950 nm) whereas the **Au(dt)$_2$** complexes absorb in the NIR-II region (1500–1700 nm). The nickel and the palladium complexes strongly absorb around 950 nm and the platinum complexes around 880 nm. The **Au(bordt)$_2$** complexes have their absorption maxima around 1500 nm and the **Aux(OCn)** complexes around 1600 nm. The maximum molar absorptivities range from 9260 to 55600 L mol^{-1} cm^{-1}. The **Mx(OCn)** complexes with M = Ni, Pd, Pt complexes are the strongest absorbers with ε_{max} varying from 38760 to 55600 L mol^{-1} cm^{-1} for **Mx(OCn)**, M = Ni, Pd, Pt. **Au(dt)2** and **Ni(dmitCn)** absorb half as much (1700–27400 L mol^{-1} cm^{-1}). Finally, **Ni4(OMe)** and **Ni4Ph** absorb much less than **Nix(OCn)**, despite their structural similarity.

The choice of metal center enables absorption maximum to be controlled over virtually the entire NIR range. The chemical modification of the diphenylethylenedithiolate ligands also allows to finely tune the λ_{max} values. The absorption wavelength can be increased by adding alkoxy chains by a few tens of nanometers, but remains invariant to changes in chain length (C4, C8 or C12 chains). Modification of the length of the carbon on a given family of complexes only affect the molar absorptivity of the complexes.

Quantitative photothermal studies have been then performed to evaluate the photothermal activities of all the dithiolene complexes. To this end, dilute solutions of all dithiolenes in toluene were irradiated with lasers at 880, 940 and 1600 nm for **Pt(dt)$_2$**, **Ni/Pd(dt)$_2$** and **Au(dt)$_2$** respectively, until they reached thermal equilibrium. By analyzing several cooling curves for each complex, photothermal efficiencies were determined with good reliability. The complexes reveal a powerful and specific photothermal effect, with elevations of several tens of degrees compared with pure solvent, as well as excellent thermal and photophysical stability. From a qualitative point of view, these compounds are therefore very promising for PTT. From a quantitative point of view, η values range from 30 to 66%. The photothermal efficiencies of the **Mx(OCn)** complexes range from 32 % to 56 % with the **Pdx(OCn)** complexes being the most efficient. The **Ni(dmitCn)** complexes have an average photothermal efficiency around 60 % and the **Au(D/DL-bordt)** are the most efficient complexes to convert light into heat. Again, **Ni4(OMe)** and **Ni4Ph** display lower values than other structurally related complexes of the **Mx(OCn)** series.

As demonstrated, the maximum temperature reached under laser irradiation is not directly correlated to the photothermal efficiencies. As

seen, some compounds displaying good photothermal conversion efficiency can generate lower temperature increases than some other complexes with lower photothermal conversion efficiency. Photothermal efficiency cannot therefore be used directly to classify photothermal agents according to their ability to convert light into heat. This is why a photothermal index, resembling luminescence brightness and taking into account both photothermal efficiency and the compound's ability to absorb light, has recently been introduced. This parameter was tested on this large library of metal-bis(dtihiolene) complexes, as well as on a perylene derivative with a completely different molecular structure. A good linear correlation was obtained between the maximum temperature reached at thermal equilibrium and the compound's photothermal index. The photothermal index can therefore be used to properly rank photothermal agents according to their ability to convert light into heat. **Mx(OCn)** complexes with M = Pt, Pd, and Ni and long carbon chains are the most efficient photothermal agents, followed by **Ni(dmitCn)**, **Aux(OCn)** complexes. Although they reach respectable maximum temperatures of around 60 °C under laser irradiation of 3 W cm^{-2}, **Ni4(OMe)**, **Ni4Ph** and **Au(D/DL-bordt)** are ultimately the least effective photothermal agents. On the basis of I_{PT} values, the following ranking can therefore be established:

Pd4(OC12) > Pd4(OC4) ≈ Pt8(OC12) ≈ Pt4(OC12) > Ni8(OC12) ≈ Ni4(OC12) ≈ Ni4(OC4) > Pd8(OC12) ≈ Pt4(OC4) > Ni(dmitC8) ≈ Ni(dmitC12) ≈ Ni(dmitC4) ≈ Au4(OC12) ≈ Au4(OC4) > Ni4(OMe) ≈ NiPh > Au(OC12) > Au(D/DL-bordt) > PerDIS.

However, the use of I_{PT} has certain limitations: i) for comparison purposes, measurements must be carried out in the same solvent, as molar absorptivity can vary depending on the nature of the solvent; ii) measurements must be carried out on the same experimental setup with a well-defined data analysis, as η values can vary depending on the sample environment and how the temperature profile is analysed [25,26]. Standardization of the methodology for measuring photothermal efficiencies, or the discovery of a photothermal standard, could therefore be a promising way of comparing photothermal agents measured worldwide, particularly with the use of the I_{PT} photothermal index.

3.1. Experimental part

Photothermal agents **M4(OC4)** [27], **M4(OC12)** [28] and **M8(OC12)** [29] have been synthesized as previously described in the literature. The parent nickel complexes **Ni4(OMe)** and **Ni4Ph** were synthesized following the same procedure from the commercially available *p*-anisil and benzil. Preparation of **Ni(dmitCn), n = 4, 8, 12**, was achieved by treatment of the corresponding 1,3-dithiole-2-thione derivative with Potassium tert-butoxide (tBuOK), followed by addition of a solution of nickel(II) chloride hexahydrate. It should be noticed that the **dmitCn** complexes could not have been isolated with the other metal center. **Au(D-bordt)** and **Au(DL-bordt)** complexes were synthesized has previously described [21]. Full synthetic details and characterization of the proligands and the metal complexes are given in Supporting Information. *N,N*-di(*n*-butyl)-1,7-dimorpholino-3,4,9,10-perylenetetrathiodiimide (**PerDIS**) was also synthesized as preciously described in the literature [22]. The purity of the compounds was ascertained by UV–Vis–NIR and NMR spectroscopies.

Toluene were provided by Carlo-Erba (FR) (Analytical grade).

UV–Vis–NIR absorption spectra in solution were recorded on a Shimadzu UV3600 Plus spectrophotometer. Samples were placed in 1 cm path length quartz cuvettes.

The molar absorption coefficients at a given wavelength (ε_λ) have been calculated using the Beer-Lambert's law: $\varepsilon_\lambda = A_\lambda/c.l$ with A_λ the absorbance at the wavelength λ, $c = 10^{-5}$ mol L^{-1} and $l = 1$ cm.

For the photothermal studies, 2 mL of solutions were irradiated through a glass cuvette with a 940 nm wavelength continuous semiconductor laser with an optical fiber (105 μm/0.22) (BWT Beijing LTD), or with 808, 880 nm or 1600 nm wavelength continuous semiconductor laser with an optical fiber (105 μm/0.22) (Changchun New Industries Optoelectronics) for 18 min. The laser power density could be adjusted externally (0–10 W). The output power was independently calibrated using an optical power meter. A thermocouple with an accuracy of ±0.1 °C connected to a PerfectPrime (model TC0520) multimeter, run and saved on computer with the dedicated software SE520, was immersed into the solution. The thermocouple was inserted at such a position that direct irradiation from the laser was avoided. The temperature was measured every 1s.

The photothermal efficiency (η) value was calculated according to the following equation described by Roper et al. based on the energy balance of the system [24].

$$\eta = (hS\Delta T_{max} - Q_{toluene}) / I \times (1\text{-}10^{-A}) \quad \text{(Equation 2)}$$

where h is the heat-transfer coefficient, S is the surface area of the container, ΔT_{max} is the maximum steady-state temperature change of the solution, I is the power of the laser and A the absorbance at 808, 880, 940 or 1600 nm. $Q_{toluene}$ was measured independently and represents heat dissipated from light absorbed with a pure toluene solution. The hS value is derived according to equation (3):

$$\tau_s = m_{toluene}C_{p\ toluene} / hS \quad \text{(Equation 3)}$$

where τ_s is the sample system time constant (in second), $m_{toluene}$ (1.73 g) and $C_{p\ toluene}$ (1.70 J $g^{-1}{\cdot}K^{-1}$) are the mass and the massic isobaric heat capacity of toluene. τ_s is given be the slope of the linear fitting from the time of the laser off state vs $-\ln(\Delta T/\Delta T_{max})$.

The solutions have been irradiated during 18 min (1080 s) which is the time needed to reach a steady state. After turning off of the laser, the cooling regime of the solutions were recorded for another 18 min.

It should be noticed that the photothermal efficiency measurement must be carried out on sufficiently diluted solutions of the photothermal agent. Indeed, if the solutions are too concentrated, it is observed that the temperature increase measured is no longer proportional to the amount of photothermal agent involved. At high concentration, the entire laser beam is absorbed by the solution, and therefore a part of the molecules present do not take part to the heat generation, i.e. lack of available photons. This results in a minimization of the maximum temperature reached and therefore an under-evaluation of the photothermal efficiency of the compound studied.

Uncertainty intervals are confidence intervals following Student's rule with α = 5 % and a number of measures N (given for each compound).

CRediT authorship contribution statement

Jean-Baptiste Pluta: Writing – review & editing, Investigation, Formal analysis. **Nathalie Bellec:** Writing – review & editing, Investigation, Conceptualization. **Franck Camerel:** Writing – review & editing, Writing – original draft, Supervision, Project administration, Investigation, Formal analysis, Conceptualization.

Declaration of competing interest

The authors declare that they have no known competing financial interests or personal relationships that could have appeared to influence the work reported in this paper.

Data availability

Data will be made available on request.

Acknowledgements

The authors thank the CNRS, the University of Rennes 1 and the "Ligue Contre le Cancer Grand Ouest" for financial support.

Appendix A. Supplementary data

Supplementary data to this article can be found online at https://doi.org/10.1016/j.dyepig.2024.112130.

References

[1] Akimov AB, Seregin VE, Rusanov KV, Tyurina EG, Glushko TA, Nevzorov VP, Nevzorova OF, Akimova EV. Nd:YAG interstitial laser thermotherapy in the treatment of breast cancer. Laser Surg Med 1998;22:257–67.

[2] Li X, Lovell JF, Yoon J, Chen X. Clinical development and potential of photothermal and photodynamic therapies for cancer. Nat Rev Clin Oncol 2020;17:383–5.

[3] Ku G, Wang LV. Deeply penetrating photoacoustic tomography in biological tissues enhanced with an optical contrast agent. Opt Lett 2005;30:507–9.

[4] Sakudo A. Near-infrared spectroscopy for medical applications: current status and future perspectives. Clin Chim Acta 2016;455:181–8.

[5] Tsai M-F, Gilbert Chang S-H, Cheng F-Y, Shanmugam V, Cheng Y-S, Su C-H, Yeh C-S. Au nanorod design as light-absorber in the first and second biological near-infrared windows for in vivo photothermal therapy. ACS Nano 2013;7:5330–42.

[6] Chen Y, Xue L, Zhu Q, Feng Y, Wu M. Recent advances in second near-infrared region (NIR-II) fluorophores and biomedical applications. Front Chem 2021;9:750404.

[7] Ali MRK, Wu Y, El-Sayed MA. Gold-nanoparticle-assisted plasmonic photothermal therapy advances toward clinical application. J Phys Chem C 2019;123:15375–93.

[8] Naief MF, Mohammed SN, Mayouf HJ, Mohammed AM. A review of the role of carbon nanotubes for cancer treatment based on photothermal and photodynamic therapy techniques. J Organomet Chem 2023;999:122819.

[9] Li R, Wang Y, Du J, Wang X, Duan A, Gao R, Liu J, Li B. Graphene oxide loaded with tumor-targeted peptide and anti-cancer drugs for cancer target therapy. Sci Rep 2021;111:1725.

[10] Cahu M, Ali LMA, Sene S, Long J, Camerel F, Ciancone M, Salles F, Chopineau J, Devoisselle J-M, Felix G, Cubedo N, Rossel M, Guari Y, Bettache N, Larionova J, Gary-Bobo M. A rational study of the influence of Mn^{2+} -insertion in Prussian blue nanoparticles on their photothermal properties. J Mater Chem B 2021;9:9670–83.

[11] Qi X, Xiang Y, Cai E, Ge X, Chen X, Zhang W, Li Z, Shen J. Inorganic–organic hybrid nanomaterials for photothermal antibacterial therapy. Coord Chem Rev 2023;496:215426.

[12] Chen P, Ma Y, Zheng Z, Wu C, Wang Y, Liang G. Facile syntheses of conjugated polymers for photothermal tumour therapy. Nat Commun 2019;10:1192.

[13] Gong L, Yan L, Zhou R, Xie J, Wub W, Gu Z. Two-dimensional transition metal dichalcogenide nanomaterials for combination cancer therapy. J Mater Chem B 2017;5:1873–95.

[14] Xiang G, Xia Q, Liu X, Wang Y, Jiang S, Li L, Zhou X, Ma L, Wang X, Zhang J. Upconversion nanoparticles modified by Cu_2S for photothermal therapy along with real-time optical thermometry. Nanoscale 2021;13:7161–8.

[15] Chen Q, Chen J, He M, Bai Y, Yan H, Zeng N, Liu F, Wen S, Song L, Sheng Z, Liu C, Fang C. Novel small molecular dye-loaded lipid nanoparticles with efficient near-infrared-II absorption for photoacoustic imaging and photothermal therapy of hepatocellular carcinoma. Biomater Sci 2019;7:3165.

[16] Shao W, Wei Q, Wang S, Li F, Wu J, Ren J, Cao F, Liao H, Gao J, Zhou M, Ling D. Molecular engineering of D–A–D conjugated small molecule nanoparticles for high performance NIR-II photothermal therapy. Mater Horiz 2020;7:1379.

[17] Dai H, Shen Q, Shao J, Wang W, Gao F, Dong X. Small molecular NIR-II fluorophores for cancer phototheranostics. Innovation 2021;2(2):100082.

[18] Ciancone M, Bellec N, Camerel F. IPT: an index to rank molecular photothermal agents. ChemPhotoChem 2020;4:5341.

[19] Camerel F, Fourmigué M. (Photo)Thermal stimulation of functional dithiolene complexes in soft matter. Eur J Inorg Chem 2020;6:508–22.

[20] Yang Y-C, Lin JS, Ni J-S. Neutral d8 metal complexes with intervalence charge-transfer transition trigger an effective NIR-II photothermal conversion for solar-driven desalination. J Mater Chem A 2023;11:26164–72.

[21] Perochon R, Poriel C, Jeannin O, Piekara-Sady L, Fourmigué M. Chiral, neutral, and paramagnetic gold dithiolene complexes derived from camphorquinone. Eur J Inorg Chem 2009:5413–21.

[22] Llewellyn BA, Davies ES, Pfeiffer CR, Cooper M, Lewis W, Champness NR. Thionated perylene diimides with intense absorbance in the near-IR. Chem Commun 2016;52:2099–102.

[23] Pluta J-B, Guechaichia R, Vacher A, Bellec N, Cammas-Marion S, Camerel F. Investigations of the photothermal properties of a series of molecular gold-bis(dithiolene) complexes absorbing in the NIR-III region. Chem Eur J 2023;29:e202301789.

[24] Roper DK, Ahn W, Hoepfner M. Microscale heat transfer transduced by surface plasmon resonant gold nanoparticles. J Phys Chem C 2007;111:3636–41.

[25] Paściak A, Pilch-Wróbel A, Marciniak Ł, Schuck PJ, Bednarkiewicz A. Standardization of methodology of light-to-heat conversion efficiency determination for colloidal nanoheaters. ACS Appl Mater Interfaces 2021;13:44556–67.

[26] Wang X, Li G, Ding Y, Sun S. Understanding the photothermal effect of gold nanostars and nanorods for biomedical applications. RSC Adv 2014;4:30375–83.

[27] Prignot E, Zhang C, Jeannin O, Halime Z, Gramage-Doria R, Camerel F. Divergent behavior in the chemistry of metal-bis(dithiolene) complexes appended with peripheral aliphatic butyl chains. Eur J Inorg Chem 2023;26:e202200591.

[28] Ohta K, Takagi A, Muroki H, Yamamoto I, Matsuzaki K, Inabe T, Maruyama Y. Novel discotic liquid crystals obtained from substituted bis(dithiolene)nickel complexes. J Chem Soc Chem Commun 1986:883–5.

[29] Ohta K, Inagaki-Oka Y, Hasebe H, Yamamoto I. Discotic liquid crystals of transition metal complexes 25: influence of the central metal on columnar mesomorphism and π-acceptor properties of the octa-alkoxy-substituted bis(diphenyldithiolene) metal complexes. Polyhedron 2000;19:267–74.